Islamic Azad University

Journal of
Optoelectronical Nanostructures

Summer 2024 / Vol. 9, No. 3

Research Paper

Efficiency Improvement of InGaP/SiGe Tandem Solar Cell Using $Si_{0.18}Ge_{0.82}$ Graded Buffer Regions

Mojtaba Shahraki[1]*, Majid Ghadrdan[1],

[1] Faculty of Electrical and Computer Engineering, University of Sistan and Baluchestan, Zahedan, Iran.

Received: 19 Feb. 2024
Revised: 20 Mar. 2024
Accepted: 1 Jun. 2024
Published: 15 Sep. 2024

Keywords:
Efficiency (*Eff*),
Graded Buffer,
Open Circuit Voltage (*Voc*),
Short Circuit Current Density (J_{sh}),

Abstract:
In this paper, the effect of SiGe graded buffers on the performance of an InGaP/SiGe tandem solar cells is investigated. It is shown that, by the proper design of graded buffer layers, the efficiency of solar cells can be improved considerably. The proposed structure consists of an InGaP top cell and a SiGe bottom cell, which are separated by a tunnel junction and a window layer. Each part has a BSF layer and graded buffers are used between window and bottom cell as well as the bottom cell and the substrate.
Different parameters of the solar cell, involving photogeneration rate, electric field and the built-in potential, are calculated. Using the PSO algorithm for the proposed solar cell, the optimized dimensions and doping are determined to reach the maximum efficiency. The short circuit current density (J_{sh}) of 21.5 mA/cm^2, Open circuit voltage (V_{oc}) of 2.14 V, efficiency (η) of 38.18% and fill factor (FF) of 83% are obtained, which show the applicable improvement compared to other works.

Citation: Mojtaba Shahraki, Majid Ghadrdan. Efficiency Improvement of InGaP/SiGe tandem solar cell using Si0.18 Ge0.82 graded buffer regions. **Journal of Optoelectronical Nanostructures. 2024; 9 (3): 1-18.**
DOI: 10.30495/JOPN.2024.33226.1313

***Corresponding author: Mojtaba Shahraki**
Address: Faculty of Electrical and Computer Engineering, Sistan and Baluchestan Universitym Daneshgah Street, Zahedan, Iran. **Tell:** 05431136549
Email: m.shahraki@ece.usb.ac.ir, mo_shahraki@yahoo.com

1. INTRODUCTION

Photovoltaic (PV) technology has noticeable benefits compared to other renewable technologies. Henceforth, the best source of energy is solar energy which is not only clean, perpetual, and environment-friendly but also copiously available [1-8]. Therefore, so many efforts are performed to make a highly efficient solar cell in order to convert the maximum sunlight to electricity [9-10]. For this purpose, great attention is paid to the devise of the III–V tandem solar cells, especially for the aerospace applications. In addition, using silicon-based dual-junction solar cells with III-V layers as top cells may bring about less expensive structures [11-13]. Recently, materials with higher absorption wavelengths have used in the design of solar cell system [14]. SiGe has unique properties including relatively high mobility, tunable lattice constant and also ability to absorb higher wavelengths up to 1800 nanometers. As a result, this material is a reasonable choice to use as the bottom cell in tandem solar cells [15-18].

In 2012, Singh et al. investigated the effects of BSF layers on the performance of InGaP/GaAs double junction solar cells [19]. They have shown by the proper design of BSF layers in terms of material and thickness, it is possible to enhance the overall efficiency of the solar cell. However their designs lack a proper current matching procedure. In 2015, a GaAsP/SiGe solar cell was proposed which utilized the silicon as the substrate. The efficiency of this structure reached up to 18.9% [20].

They have used a graded SiGe layer between the bottom cell and Si substrate. This layer provided matching condition between the substrate and bottom cell. However, this matching layer was not used between other layers.

In 2016 a GaAs/SiGe tandem sola cell is designed which have used the silicon as the substrate [21]. The efficiency of this structure have reached to 20.6%.They have also used the graded layer only between the bottom cell and the substrate.

One year later, a GaAsP/SiGe tandem solar cell is designed by Zhao et al. which had the efficiency up to 24.4 % [22]. In their work, by optimization of the fabrication process and device structure, the short-circuit current density is increased from 12.9mA/cm^2 to 19.4mA/cm^2. Also, the efficiency of the SieGe bottom cell is improved from 1.7% to 3.0% filtered by GaAsP. However, the focus of their study was on the graded layer between SiGe and Si layer and the optimal design of BSF and window layers lacks in their experiments.

Other papers have tried to improve the efficiency of the solar cells by some adjustment to different layers. For example in [23] and [24] a double BSF layer is used in the top cell of solar cell. BSF layers design can reduce the

recombination between the top call and tunnel junction as well as the tunnel junction and the substrate.

Using double layers can improve this passivation and incorporate to efficiency improvement of the solar cell .However, no graded layer is used in their structure and instead the materials are selected by the lattice constant, which limits the selection choices.

In 2020 Cano et al. have used the combination of Ge and graded SiGe layers on the Si substrate to improve the lattice matching of the bottom cell with the substrate [25]. Similar approach is used in 2023 by Kim et al. for an AlGaAs bottom cell [26]. Graded SiGe on Ge layers can provide a smooth transition from bottom cell to substrate. Once again no graded layer is used in these studies for the top cell and a matched composition is selected which limits the choices for the top cell material.

In this paper, a tandem solar cell based on IBGaP/SiGe is proposed which GaAs is selected as the substrate. Two graded layers are used between top cell and bottom cell and bottom cell and substrate as well. This provides a smooth transmission between layers and ensures the lattice matching throughout the whole solar cell. Also, double BSF layers are used in both the top and bottom cell to increase passivation and improve the overall efficiency of the solar cell. Tunnel junction is used between two cells to transmit the carriers throughout the barriers. The remainder of this paper is organized as follow: in part 2 the proposed solar cell structure is presented. In this part we focus on the arrangement and material of the different layers. In part 3 performance parameters are studied and how these parameters can be obtained. In part 4 results are presented and these results are discussed and compared to previous studies, before concluding the paper.

2. THE ARRANGEMENT OF THE PROPOSED STRUCTURE

The proposed tandem solar cell is constituted of different layers. It consists of three major parts. First the top cell is considered. This cell consists of a window layers, an InGaP p–n diode, and the BSF layer. Next part is a tunnel junction between two cells. Finally a bottom cell is used which consists of a window layer, a SiGe p–n junction, another BSF layer and the finally the buffer layers, which are graded in our design.

Because of high absorption in the active layer of solar cells, photons are absorbed near the surface of the solar cell, where recombination can be substantial. A window layer with a large bandgap is deployed to minimize the front surface recombination.

In a dual junction solar cell, the window layer should have a higher bandgap than the following layers. Also, compared to the emitter layer, its bandgap energy should be high. It also must impart a potential barrier to prevent the flowing of the minority carriers of the emitter [8].

The BSF lasers can act as the passivation layer between the tunnel junction and the top cell and bottom cell or the substrate. Moreover, they have a relatively higher bandgap which helps on reducing the scattering of charge carriers and improving the overall efficiency of the solar cell [27]. Here, we have used two different layers as BSF in top cell as well as the bottom cell.

The tunnel diode layer must deliver a low resistance pathway for charge carriers to move between the bottom and top cells [8], [27]. They are essential in the design of tandem solar cells which must be transparent and also have a low resistant. In the present model, InGaP material is used for the tunnel diode region, and the energy band diagram is obtained according to this assumption.

In this paper, all the properties of the materials are taken from [19], [33] and [34]. In simulations, the AM1.5G is used as the source [30]. The proposed structure is presented in Fig.1 and Table 1 shows the material parameters which are used in our simulations.

The proposed structure is a tandem solar cell consisting of InGaP at top and InGaP at the bottom that is located on GaAs substrate. An InGaP tunnel junction is used between two cells.

The material of the upper cell must have the higher bandgap to absorb the more energetic parts of the sunlight. In this study, InGaP is used as the upper cell, which has the bandgap of aroudd 1.86-1.9eV [31-32]. The less energetic parts of the sunlight will transmit through this cell and reaches to the bottom cell. SiGe (0.86-0.98eV) is used as narrow bandgap material in the lowest cell. It absorbs higher wavelengths of the sunlight up to 1800 nm [21], [22] and [33]. Tunnel junctions are employed between the top and bottom parts of the solar cell. Transports of carriers are facilitated by this junction between the cells.

Material of Anode and Cathode are selected as aluminum which are more suitable for these structures and can be made straightforward by annealing processes [21]. The doping of different layers is selected from experimental studies which are displayed in Table 1. In practice, the doping of BSF layer can be varied from 2e17 [23] and 5e18 [19] to 5e19 [14]. We have used the doping of BFS layers in these ranges and changed it to reach the best results. In our studies, the doping of substrate is selected as 2e18. It is worth noting that sometimes the doping of the substrate reduced to improve the electric field for collecting the carriers [21]. However, this requires special techniques and considerations in practice to avoid Schottky contact formation. Moreover, it has negligible effects on the final efficiency of the solar cell.

As a result and to avoid these practical complexities we set the doping of this layer to 2.3e18. Heavily doped window layers used on top of the solar cell provide a low top contact resistance. The doping of other layers are selected by the optimization algorithms, which is discussed later in part 4.

Anode			
Window 1	$In_{0.5}(Al_{0.7}Ga_{0.3})_{0.5}P$	0.04µm	p=7.5e18cm^{-3}
Window 2	$In_{0.5}(Al_{0.7}Ga_{0.3})_{0.5}P$	0.03µm	p=2.2e18cm^{-3}
Emitter	$In_{0.49}Ga_{0.51}P$	0.06µm	p=2.2e18cm^{-3}
Base	$In_{0.49}Ga_{0.51}P$	0.54µm	n=6.8e16cm^{-3}
BSF1	$In_{0.5}(Al_{0.7}Ga_{0.3})_{0.5}P$	0.03µm	n=2.9e18cm^{-3}
BSF2	$In_{0.5}(Al_{0.7}Ga_{0.3})_{0.5}P$	0.03µm	n=4.1e18cm^{-3}
Tunnel Diode	$In_{0.49}Ga_{0.51}P$	0.025µm	n=9.2e19cm^{-3}
Tunnel Diode	$In_{0.49}Ga_{0.51}P$	0.025µm	p=8.1e19cm^{-3}
Window	GaAs	0.06µm	p=3.6e18cm^{-3}
Graded Buffer	$Si_{1-x}Ge_x$	0.08µm	p=2.3e18cm^{-3}
Emitter	$Si_{0.18}Ge_{0.82}$	0.48µm	p=2.3e18cm^{-3}
Base	$Si_{0.18}Ge_{0.82}$	4µm	n=2.3e17cm^{-3}
BSF1	$Si_{0.18}Ge_{0.82}$	0.05µm	n=2.3e18cm^{-3}
BSF2	$Si_{0.18}Ge_{0.82}$	0.04µm	n=2.3e19cm^{-3}
Graded Buffer	$Si_{1-x}Ge_x$	0.48µm	n=2.3e18cm^{-3}
Substrate	GaAs	2.2µm	n=2.3e18cm^{-3}
Cathode			

Fig. 1. The proposed InGaP/SiGe tandem solar cell.

TABLE I
PARAMETERS FOR DIFFERENT MATERIALS.

Material parameter	$In_{0.49}Ga_{0.51}P$	$In_{0.5}(Al_{0.7}Ga_{0.3})_{0.5}P$	GaAs	$Si_{0.18}Ge_{0.82}$
Band gap (eV)	1.9	2.3	1.42-1.45	0.781
Lattice Constant ($Å$)	5.65	5.65	5.65	5.43
Relative Permittivity (ε_r)	11.6	11.7	13.1	15.8
Affinity (eV)	4.16	4.2	4.07	4.02
e-mobility (μ_n) (cm^2/Vs)	1945	2150	8800	1430
h-mobility(μ_p) (cm^2/Vs)	141	141	400	480
e-lifetime (S)	1e^{-9}	1e^{-9}	1e^{-9}	3e^{-5}
h-lifetime (S)	1e^{-9}	1e^{-9}	2e^{-8}	1e^{-5}
n_i ($per\ cc$)	7.44e^{+4}	1	2.13e^{+6}	3.51e^{+12}

3. PERFORMANCE PARAMETERS

In this part, some parameters are taken into attention. According to these parameters, one can reflect on the practicality of the proposed structure:

A. Short circuit current (I_{sh})

Two different sources are existed in the solar cells, including dark current and the current generated at the presence of light. The final current (I_{total}) can be obtained as the summation of these two currents [8].

$$I_{total} = I_0[\exp(\frac{qV}{nkT}) - 1] - I_L \quad (1)$$

where n accounts as the ideality factor, I_0 is the saturation current, T is temperature (by Kelvin), q is the charge of electrons, and k is Boltzmann's constant (kT/q). Now to get I_{sh}, we put the condition V=0:

$$I_{sh} = -I_L \quad (2)$$

where normally I_{sh} can be written in terms of current density ($J_{sc}=I_{sh}/A$) where it has the unit of A/cm^2.

B. Open circuit voltage (V_{oc})

By putting the condition (I=0) in Eq. (1), we can obtain the V_{oc}, that is, the voltage produced across the two terminals of the solar cell when no current is flowing [27].

$$V_{oc} = \frac{nkT}{q}\ln(\frac{I}{I_0} + 1) \quad (3)$$

C. *Fill factor (FF)*

The fill factor can be obtained as the maximum power generated by the solar cell, divided by the $V_{oc.}$ I_{sc} which is the ideal power [27]. This parameter is a representative of the squareness and subsequently ideality of the I–V cure.

$$FF = \frac{I_m V_m}{I_{sc} V_{oc}} = \frac{\frac{qV_{oc}}{nkT} - \ln(\frac{qV_{oc}}{nkT} + 0.72)}{\frac{qV_{oc}}{nkT} + 1} \quad (4)$$

Here V_m and I_m are the voltage and current where the maximum power is reached.

D. Efficiency (η)

The efficiency is a measure of how much of the incident power is absorbed in the solar cell which is described as the ratio of the power generated by the solar cell to the power impinged on the solar cell by the sunlight and cab be written as:

$$\eta = \frac{V_{oc} I_{sc} FF}{P_{in}} \tag{5}$$

where P_{in} is the input power and indicates the incident sunlight power which is equal to 1000 W/cm^2 [8].

4. OPTIMIZATION OF THE STRUCTURE

Here, we have used the particle swarm optimization (PSO) algorithm to find the best possible structure. The efficiency of the solar cell is used as the objective function and dimensions and doping of each layer are selected as the input parameters for the PSO algorithm. As a result, the best parameters can be selected to reach the maximum efficiency of the solar cell. The range of input parameters to be used in the optimization processes are selected around the choices of the previous studies [19] [33-34].

The PSO algorithm starts by preparing a population of randomly produces parameters called particles and modifies these particles in the search-space based on pre-determined processes. In each repetition, the algorithm examines for the best position by updating production through the velocity and position update equations [33]. Updating of each particle is influenced by its local best determined position and also it is directed to the global best determined position in the search-space. If a better position is discovered in each iteration, both of the local and global positions are updated.

One important parameter is the convergence criteria, which in this paper is chosen to be the particular number of iterations and the maximum numbers of iterations are set to 300 times. Also the population of particles is set to 150. In order to prevent the algorithm to tumbling into local optima, mutation is performed in each iteration, which means producing new particles by mutation processes.

The flowchart of this process for our simulations is displayed in Fig. 2.

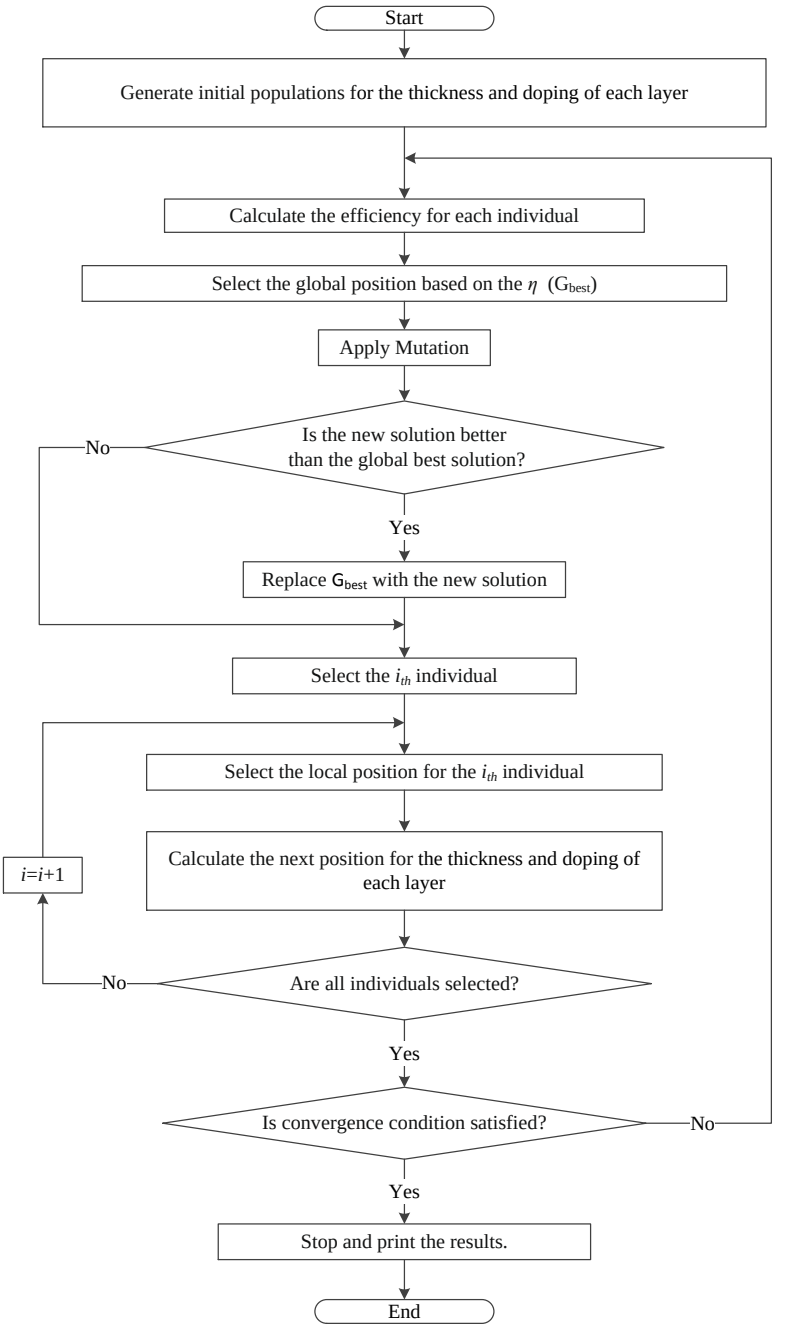

Fig. 2 Flowchart of the PSO algorithm for our structure.

5. SIMULATION AND DISCUSSIG THE RESULTS

Here, the full descriptions of the different results are considered. In our simulations, auger recombination, radiative recombination, surface recombination, Shockley-read-hall recombination, Fermi-Dirac statistics, concentration-dependent mobility, non-local band-to-band tunneling, and bandgap narrowing are taking to account.

Details of these models are cumbersome and can be found in the literature [7]. AM1.5G spectrum is used as the input on top of the solar cell. Fig. 3 shows electrical potential developed in each layer of the proposed tandem solar cell.

As can be realized in the tunnel junction, the electrical potential is maximized. This is a result of the high built-in potential in this junction. The highest potential exists in the tunnel junction which helps to transmit carriers across the junction.

Another important parameter is the photogeration which shows the amount of the photons produced in each part of the solar cell in the presence of sunlight. Higher photogeneration rates can provides higher efficiencies by increasing the photocurrent across the solar cell. Photogeneration of the solar cell is directly obtained by absorption of the light inside the solar cell.

Fig. 4 demonstrates the photogeneration rate through the structure. It is shown that a photogeneration rate is maximum at the top of the solar cell because it receives the maximum sunlight.

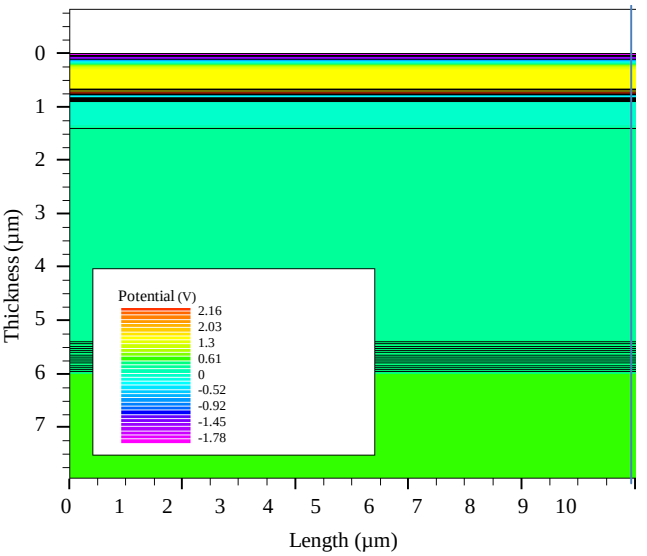

Fig. 3. Electrical potential created in each layer of the proposed tandem solar cell

In addition, due to presence of BSF layers, the scattering of the carriers is minimized, which leads to a higher ratio of photogeneration.

As seen in Fig. 3, the potential for tunnel junction is higher than for other junctions that lead to the electric field in that junction being higher than the other junctions. The generated electric field of each layer of the proposed solar cell is shown in Fig. 5. The resulting field across the tunnel junction is high enough to contribute in drifting the collected carries across the junction and improvement of the final efficiency of the solar cell.

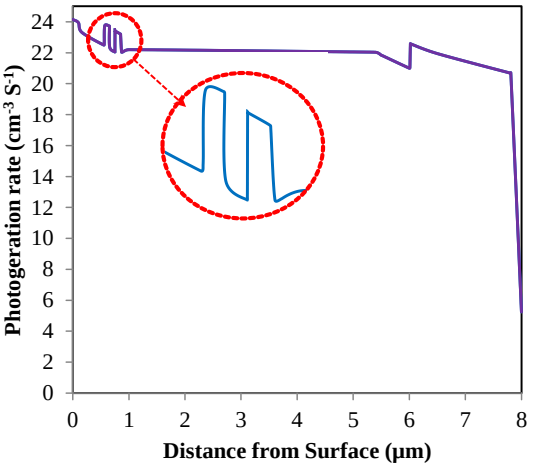

Fig. 4. Photogeneration rate in the proposed solar cell.

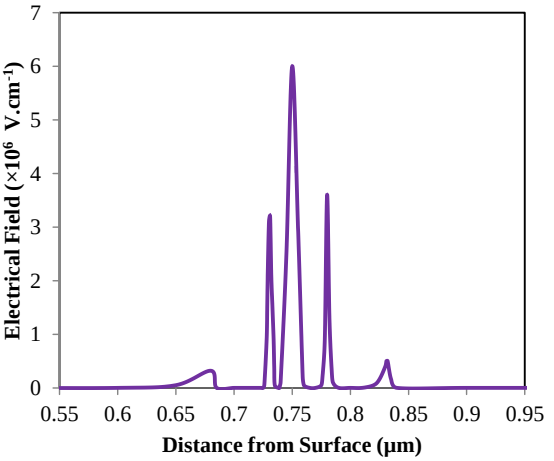

Fig. 5. Electric field established through the solar cell across the tunnel junction.

The dimensions are in accordance to the Fig.1 which is started from the top of the solar cell as zero. This Figure only focuses on the range of the 0.65 to 0.85 micrometer where the tunnel junctions are existed.

The objective of this picture is to underline the effects of tunnel junctions for tunneling the carriers through the layers. Since it was not the focus of our study, the field at the beginning and end of the device is not shown in this figure.

However the doping of p-n junctions at the base and emitter in each layer can ensure the strong enough fields for the collection of carriers at the terminals. However, these fields are not comparable to the tunnel junctions where the tremendous electric fields are required.

In Fig. 6, the power curve in the solar cell model is shown. Using the power curve, one can obtain the maximum power density of the solar cell.

The maximum power density for our structures is calculated to be 38.11 mW/cm^2 which is related to the voltage of 1.96 V.

This power leads to the fill factor (FF) of 83, which is higher than previously reported data for dual junction solar cells. One important aspect of the proposed structure is the shifting of the maximum power point toward the higher voltages that will contribute to the better utilization of the collected carriers.

Finally, the J-V curve of the proposed tandem solar cell system is presented in Fig. 7. It displays the short circuit current density of 21.5 mA/cm^2 and open-circuit voltage of 2.14 V for the proposed structure. The fill factor of the proposed structure can be calculated from this picture as well, which is 83 percent.

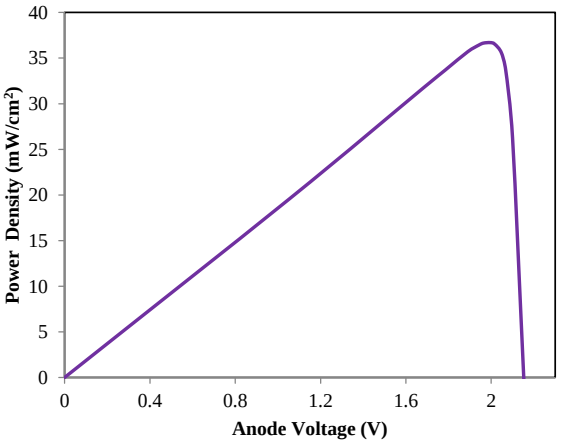

Fig. 6. Power curve generated for the dual junction solar cell.

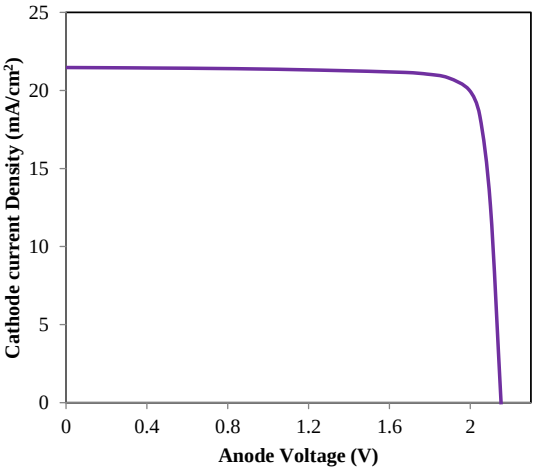

Fig. 7. J-V curve of the proposed solar cell.

A. Major solar cell performance comparison

The results are obtained in this paper are compared to Refs [20], [21] and [33] which is displayed in Table 2. As can be seen from the evaluation of these values, the results from this structure have improved significantly.

B. Discussion

Although our structure shows improvement considering the overall efficiency of the solar cell, there are some concerns that must be addressed before concluding the paper. First, it must be mentioned that we have used a perfect regular pattern for graded SiGe layers. In fact we have assumed that the 0.48μm graded layer consists of 48 layers where the x composition changes linearly across each layer. This could be different from the practical graded layers which lead to the different outcome. In fact the real graded junction can be made by different techniques, including liquid phase epitaxy [34]. All growth begins from the identical temperature but finishes at diverse ultimate temperatures.

TABLE 2
COMPARISON OF THE RESULTS.

Reference	*Jsc* (mA/cm^2)	V_{OC} (*V*)	Fill Factor	Efficiency (%)
[26]	19.6	1.19	79	18.4
[27]	18.1	1.45	71	18.6
[33]	18.6	1.43	81	21.5
This paper	21.5	2.14	83	38.18

The original film growth is fully strained as the growth continues, it becomes fully relaxed. This could limit the performance of the proposed structure which benefits from two graded layers between cells and substrate. One way to reduce the cracks during the fabrication of graded layers is to use porous substrate [35]. Using this method could also change the overall characteristics of the solar cell, as well. Another important issue is the thickness of different layers.

It must be noticed that the thicknesses of around 0.025μm which is used in tunnel junctions cannot be achieved easily and precisely in the fabrication process, especially when the high doping are needed for these layers. This could also diminish the final efficiency of proposed the solar cell in practice. The other subject relates to the simulation models. In our simulations we have tried to consider all the possible models in the cells and tunnel junctions including Auger, direct and Shockley-Read Hall recombination.

However, the surface recombination is not considered in our simulations. Even by the proper passivation at the front end of the solar cell, some recombination may occur at the top of solar cell and the final current density of the solar cell will diminish slightly compared to the simulations. In summary, the proposed design promises a considerable improvement compared to previously reported designs. However, more studies on the practical and fabrication challenges are needed.

6. CONCLUSION

In this paper, a tandem solar cell consisting of InGaP/SiGe is suggested, and the effects of two $Si_{0.18}$ $Ge_{0.82}$ based graded buffer regions and optimized $Si_{0.18}$ $Ge_{0.18}$ base layer is analyzed. The proposed structure showed impressive performance according to its efficiency (η). By using two $Si_{0.18}$ $Ge_{0.82}$ based graded buffer regions and optimizing the $Si_{0.18}$ $Ge_{0.82}$ base layer, a better photoabsorption of solar radiation is performed. The efficiency of the solar cell is found to be 38.11 % and V_{oc}, J_{sh} and for this structure are calculated as 2.14 V and 21.5 mA/cm^2, respectively. The J_{sh}, V_{oc}, and efficiency show a significant increase of about 1.83%, 0.68%, and 16.22% than mentioned in [16].

REFERENCES

[1] M. Amirhoseiny, M. Zandi, A. Kheiri, *A comparative study of BSF layers for InGaN single-junction and multi-junction solar cells*. journal of optoelectronical nanostructures. 9(1) published online (2024). https://jopn.marvdasht.iau.ir/article_6220.html

[2] A. Mahmoudloo, *Investigation and Simulation of Recombination Models in Virtual Organic Solar Cell*. journal of optoelectronical nanostructures.7(4) (2022) 1-12.
https://jopn.marvdasht.iau.ir/article_5674.html

[3] S. R. Hosseini, M. Bahramgour, N. Delibas, A. Niaei. *A simulation study around investigating the effect of polymers on the structure and performance of a perovskite solar cell*. journal of optoelectronical nanostructures, 7(2) (2022) 37-50.
https://jopn.marvdasht.iau.ir/article_5264.html

[4] M. rajaee, S. Rabiee. *Analysis and Implementation of a New Method to Increase the Efficiency of Photovoltaic Cells by Applying a Dual Axis Sun Tracking System and Fresnel Lens Array*. journal of optoelectronical nanostructures. 6 (3) (2021) 59-80.
https://jopn.marvdasht.iau.ir/article_4981.html

[5] R. yahyazadeh, Z. hashempour. *Effect of Hydrostatic Pressure on Optical Absorption Coefficient of InGaN/GaN of Multiple Quantum Well Solar Cells*. journal of optoelectronical nanostructures. 6(2) (2021) 1-22.
https://jopn.marvdasht.iau.ir/article_4768.html

[6] S. Fonash, *Semiconductor–semiconductor Heterojunction Cells*, in Solar Cell Device Physics, 2nd ed., United States of America, Academic Press, Elsevier, 2010, 183-262.
https://www.sciencedirect.com/book/9780123747747/solar-cell-device-physics

[7] A. Goetzberger, J. Knobloch, and B. Voß, *The Physics of Solar Cells*, in Crystalline Silicon Solar Cells, Chichester, UK, John Wiley & Sons, 2014, 67–86.
https://www.wiley.com/en-us/Crystalline+Silicon+Solar+Cells-p-9780471971443

[8] A. Luque and S. Hegedus, *The Physics of the Solar Cell*, in Handbook of Photovoltaic Science and Engineering, vol. 1. Chichester, UK, John Wiley & Sons, 2003.
https://onlinelibrary.wiley.com/doi/book/10.1002/0470014008

[9] M. R. Salehi, M. Shahraki. *Circuit modeling of waveguide grating nanostructures in ultrathin solar cells*. IEEE Transactions on Nanotechnology, 16(4) (2017) 616-623. https://ieeexplore.ieee.org/document/7912409

[10] S. L. Mortazavifar, M. R. Salehi, M. Shahraki. *Ultrathin nano-ring metasurface absorber in visible regime based on circuit model*. The European Physical Journal Plus. 137(9) (2022) 1072. https://epjplus.epj.org/articles/epjplus/abs/2022/09/13360_2022_Article_3272/13360_2022_Article_3272.html

[11] A. Willoughby and G. Conibeer, *Solar Cell Materials: Developing Technologies*, 1st ed. Chichester, UK: John Wiley & Sons, 2014. https://www.wiley.com/en-us/Solar+Cell+Materials%3A+Developing+Technologies-p-9781118695814

[12] K. Gledhill. *High-efficiency multi-junction space solar cells*. presented at the Space Programs and Technologies Conference, 32 (1995) 1-4. https://arc.aiaa.org/doi/10.2514/6.1995-3540

[13] L. Fara and M. Yamaguchi, *Advanced Solar Cell Materials, Technology, Modeling, and Simulation.* IGI Global, (2013). https://www.igi-global.com/book/advanced-solar-cell-materials-technology/63885

[14] G. S. Sahoo and G. P. Mishra. *Effective use of spectrum by an ARC less dual junction solar cell to achieve higher efficiency: A simulation study*. Superlattices and Microstructures, 109 (2017) 794–804. https://www.sciencedirect.com/science/article/abs/pii/S0749603617309175

[15] R. Oshima, M. Yamanaka, H. Kawanami, I. Sakata, and K. Matsubara. *Fabrication of 0.9 eV bandgap a-Si/c-Si1-xGe1-x heterojunction solar cells* presented at the 2014 IEEE 40th Photovoltaic Specialist Conference (PVSC), (2014) 0202–0205. https://ieeexplore.ieee.org/document/6925575

[16] A. Aissat, F. Benyettou, S. Nacer, and J. P. Vilcot. *Modeling and*

simulation of solar cells quantum well based on SiGe/Si. International Journal of Hydrogen Energy. 42(13) (2017) 8790–8794. https://www.sciencedirect.com/science/article/abs/pii/S0360319916308114

[17] A. K. Singh, J. Tiwari, A. Yadav, and R. K. Jha, *Analysis of Si/SiGe Heterostructure Solar Cell*. Journal of Energy, 2014 (2014) 1–7. https://www.hindawi.com/journals/jen/2014/946406/

[18] E. Polyzoeva, S. Abdul Hadi, A. Nayfeh, and J. L. Hoyt. *Reducing optical and resistive losses in graded silicon-germanium buffer layers for silicon based tandem cells using step-cell design*. AIP Advances. 5(5) (2015) 057161. https://pubs.aip.org/aip/jap/article-abstract/119/7/073104/142365/Theoretical-efficiency-limit-for-a-two-terminal?redirectedFrom=fulltext

[19] K. J. Singh, S. K. Sarkar. *Highly efficient ARC less InGaP/GaAs DJ solar cell numerical modeling using optimized InAlGaP BSF layers*. Optical and Quantum Electronics. 38(4) (2012) 1-20. https://link.springer.com/article/10.1007/s11082-011-9499-y

[20] M. Diaz et al., *Tandem GaAsP/SiGe on Si solar cells*. Solar Energy Materials and Solar Cells. 143 (2015) 113–119. https://www.sciencedirect.com/science/article/abs/pii/S0927024815003025

[21] L. Wang et al. *Current matched three-terminal dual junction GaAsP/SiGe tandem solar cell on Si*. Solar Energy Materials and Solar Cells. 146 (2016) 80-86. https://www.sciencedirect.com/science/article/abs/pii/S0927024815006212

[22] X. Zhao et al. *Short circuit current and efficiency improvement of SiGe solar cell in a GaAsP-SiGe dual junction solar cell on a Si substrate*. Solar Energy Materials and Solar Cells, 159 (2017) 86–93, https://www.sciencedirect.com/science/article/abs/pii/S0927024816303282

[23] J. P. Dutta, P. P. Nayak, G.P. Mishra, *Design and evaluation of ARC less InGaP/GaAs DJ solar cell with InGaP tunnel junction and optimized double top BSF layer*. Optik, 127 (2016) 4156–4161.

https://www.sciencedirect.com/science/article/abs/pii/S0030402616000905

[24] G.S. Sahoo, G.P. Mishra, *Effective use of spectrum by an ARC less dual junction solar cell to achieve higher efficiency: A simulation study*. Superlattices and Microstructures. 109 (2017) 794-804. https://www.sciencedirect.com/science/article/abs/pii/S0749603617309175

[25] P. Cano, M. Hinojosa, H. Nguyen, et al., *Hybrid III-V/SiGe solar cells grown on Si substrates through reverse graded buffers*. Solar Energy Materials and Solar Cells. 205 (2020) 110246. https://www.sciencedirect.com/science/article/abs/pii/S0927024819305756

[26] E. Kim, M. A. Madarang, E. Ju, et al., *GaAs/Si Tandem Solar Cells with an Optically Transparent InAlAs/GaAs Strained Layer Superlattices Dislocation Filter Layer*. Energies. 16 (2023) 1158. https://www.mdpi.com/1996-1073/16/3/1158

[27] NJ. Hoboken , Solar Cells and their Applications, John Wiley & Sons, Inc., 2010. https://www.wiley.com/en-us/Solar+Cells+and+Their+Applications%2C+2nd+Edition-p-9780470446331

[28] E. D. Palik, Handbook of Optical Constants of Solids, Academic Press, 1998. https://www.sciencedirect.com/book/9780125444224/handbook-of-optical-constants-of-solids

[29] G. S. Sahoo, P. P. Nayak, and G. P. Mishra. *An ARC less InGaP/GaAs DJ solar cell with hetero tunnel junction.* Superlattices and Microstructures. 95 (2016) 115–127. https://www.sciencedirect.com/science/article/abs/pii/S0749603616301975

[30] C. A. Gueymard, D. Myers, and K. Emery *Proposed reference irradiance spectra for solar energy systems testing*. Solar Energy. 73 (6) (2016) 443–467. https://www.sciencedirect.com/science/article/abs/pii/S0038092X03000057

[31] J. W. Leem, Y. T. Lee, and J. S. Yu. *Optimum design of InGaP/GaAs dual-junction solar cells with different tunnel diodes*. Optical and Quantum Electronics, 41(8) (2009) 605–612. https://link.springer.com/article/10.1007/s11082-010-9367-1

[32] N. Jain and M. K. Hudait. *Design of metamorphic dual-junction InGaP/GaAs solar cell on Si with efficiency greater than 29% using finite element analysis* presented at the 38th IEEE Photovoltaic Specialists Conference, (2012) 002056–002060. https://ieeexplore.ieee.org/document/6318003

[33] L. Wang et al. *Material and Device Improvement of GaAsP Top Solar Cells for GaAsP/SiGe Tandem Solar Cells Grown on Si Substrates*. IEEE Journal of Photovoltaics, 5(6) (2015) 1800–1804. https://ieeexplore.ieee.org/document/7194733

[34] J. Wang, Y.-J. Shen, N. Quitoriano. *Growth evolution of SiGe graded buffers during LPE cooling process*. Journal of Crystal Growth, 502(15) (2018) 54-63. https://www.sciencedirect.com/science/article/abs/pii/S0022024818304068

[35] P. Caño, M. Hinojosa, I. García, et al. *GaAsP/SiGe tandem solar cells on porous Si substrates*. Solar Energy. 230 (2021) 925-934. https://www.sciencedirect.com/science/article/abs/pii/S0038092X21009385